

# Characteristics of NICMOS Detector Dark Observations.

---

C. J. Skinner, L. Bergeron  
October 14, 1997

---

## ABSTRACT

*This ISR describes the characteristics of the 'dark current' for the NICMOS flight detectors, namely the instrumental signal present in exposures made in the absence of any external illumination. We show how this comprises three distinct components - the shading, amplifier glow, and the true dark current. Each of these three components is described, and examples from the on-orbit observations are presented. We then describe a recipe for generating 'synthetic' dark current calibration reference files, which could in principle be used to generate darks for any arbitrary sequence of MULTIACCUM reads, and present results of a comparison of such a synthetic dark with observed data. Finally we describe the deficiencies that are still present in our understanding of the properties of NICMOS detector darks.*

---

## 1. Introduction

Each readout of a NICMOS detector includes not only the desired detected signal, but also the signatures of the detector itself and the readout electronics, which would be present in the signal recorded during any exposure, even in the absence of any external illumination. These parts of the output signal must be removed to get the true detected signal. In CCD cameras the only such signal is, in general, the dark current. This is a continuous feed into the pixels of electrons which are not stimulated by photons, and the total charge accumulated in an exposure is linearly dependent on exposure time. This signal is not subject to modulation by the detector non-linearity or flat-field response. Thus in a calibration of an image from a CCD, the dark subtraction must be among the first steps.

In the case of NICMOS detectors, the darks are considerably more complicated, with contributions from a number of sources. Additionally, it is possible to read the detectors non-destructively, and so it is possible to see the signal accumulating in each pixel during the course of an observation. However, the act of reading the detector in fact has a small effect on the signal. As a result of these complications, a significant 'folklore' has been

established among ground-based users of NICMOS detectors. One of the elements of this tradition is the belief that to calibrate a NICMOS exposure, it is essential to obtain a ‘dark’ (i.e. unilluminated) exposure matched exactly in number of readouts and timing of all the readouts. One of the results of this tradition is the sets of MULTIACCUM readout sequences with fixed readout times which have been offered to NICMOS observers.

Although we will show in this ISR that this is not in fact true, it is true that NICMOS darks are highly dependent on the readout history of the array since it was last reset (when all pixels were last shorted to empty the potential wells). As a result, a dark image taken for a given exposure time cannot simply be scaled by its exposure time and applied to other data (as is done with most conventional CCD data). Instead it is necessary, when constructing a ‘dark’ calibration reference file, to account properly for the three components listed earlier, each of which has a different set of dependencies.

During SMOV and Cycle 7 NICMOS operations, an effect known as the ‘pedestal’ has come to light. This is a change in the bias of the detector which is time-dependent, and appears to be related to periods of detector inactivity. This has degraded the quality of the calibration of much early NICMOS data, and has prompted a recent Flight Software change in an attempt to remove the effect. All of the results presented in this ISR derive from observations made before this change. However, although some of the numerical details have changed, the basic characteristics of the darks and their behaviour have not been altered, and so the information presented in this ISR is still applicable. Details of the pedestal will be given in a forthcoming ISR.

We describe the three components of a NICMOS dark in the next section. Throughout this ISR, when we refer to a ‘dark’ this implies an observation with no external illumination; when we refer to the ‘linear dark current’, this implies that component of the dark which is linearly dependent on time and directly analogous to the dark current of a CCD.

## **2. Components of a NICMOS dark**

### ***Amplifier Glow***

A NICMOS detector is a continuous single slab of HgCdTe, pixelated such that each pixel is individually bump-bonded to a single pixel of a CCD which is used as a readout. However, there are four separate readout amplifiers, each of which addresses one quadrant of the detector. Each time the detector is read out, the readout amplifiers, which are situated near the corners of the detector, are turned on. These amplifiers emit IR radiation that is detected by the pixels in the detector - similar to having a small “light bulb” in each corner. This produces a pattern of light that is highest in the corners and decreases towards the center of the detector. This is known as ‘amp glow’.

A typical single readout produces about 20-30 ADUs of amp-glow per pixel in the corners of the detector, and 2-3 DN near the center. Since the readout time of the detector is the

same each time (it takes 0.203 seconds to read the whole image), the on-time for the amplifiers is always the same for each readout, and thus the light pattern seen by the array is repeatable. So in a given readout, the amount of signal due to amp-glow in each pixel scales directly with the number of readouts since the last reset:

$$A(i,j) = a(i,j) * n_r$$

Where  $A(i,j)$  is the observed signal due to amp-glow in a given readout for pixel  $i,j$ ,  $a(i,j)$  is the amp-glow signal per readout (different for each pixel), and  $n_r$  is the total number of readouts of the array since the last reset. So in the corners of a full 26-readout MULTI-ACCUM there will be of order 500-800 ADUs due to amp-glow, along with the expected Poisson noise from this signal. It can immediately be seen from the size of this signal that making excessive numbers of readouts during a MULTIACCUM exposure is harmful to the results, because although the amp-glow signal is highly reproducible and can be subtracted very effectively, the Poisson noise added by it can significantly degrade the S/N of the resulting image, even close to the center of the detector where the amp-glow signal is at its minimum.

Of course, since the amp-glow is a radiation source detected by the detector, it is subject to the non-linearity and DQE characteristics of the detector. The low-level non-linearity of the NICMOS flight detectors has not been characterized yet, and such errors in making a good analytic amp-glow correction may be noticeable. Once known, non-linearity can be factored into the equation for a dark, but of course unknown source signal in science data images may make it nearly impossible to know how the amp-glow truly behaved in a given image. This effect will in most cases be small though.

### ***Shading***

The bias level, or ‘DC offset’, in a given pixel in a NICMOS array, is time- dependent. This is the so-called ‘shading’, which visually in an uncorrected image looks like a ripple and gradual signal gradient across a given quadrant. The pixels in a given quadrant of a NICMOS detector are read out sequentially. It takes a little over a  $\mu$ sec to read a single pixel, and so with four readout amplifiers reading in parallel it takes just over 0.2 sec to read the entire 256x256 pixel detector. Considering a quadrant as an array of  $i \times j$  pixels, the readout sequence consists of reading sequentially along a detector row  $i$ , clocking  $j$  from 1 to 128, then moving to row  $i+1$  and clocking  $j$  from 1 to 128, and so on. Since the amplifier bias changes pseudo-exponentially with time over the course of the readout, the observed signal, in the absence of any external illumination, varies rather slowly along the rows ( $i$ , referred to as the slow clocking direction), but rather rapidly along the columns ( $j$ , referred to as the fast clocking direction). This signal is not accumulated in the pixels during each DELTATIM period, but rather is superimposed on the actual signal at the time of each detector readout. An example shading signal is shown in Figure 1, where we show its amplitude across the Camera 2 detector, with the fast and slow clocking directions

indicated.

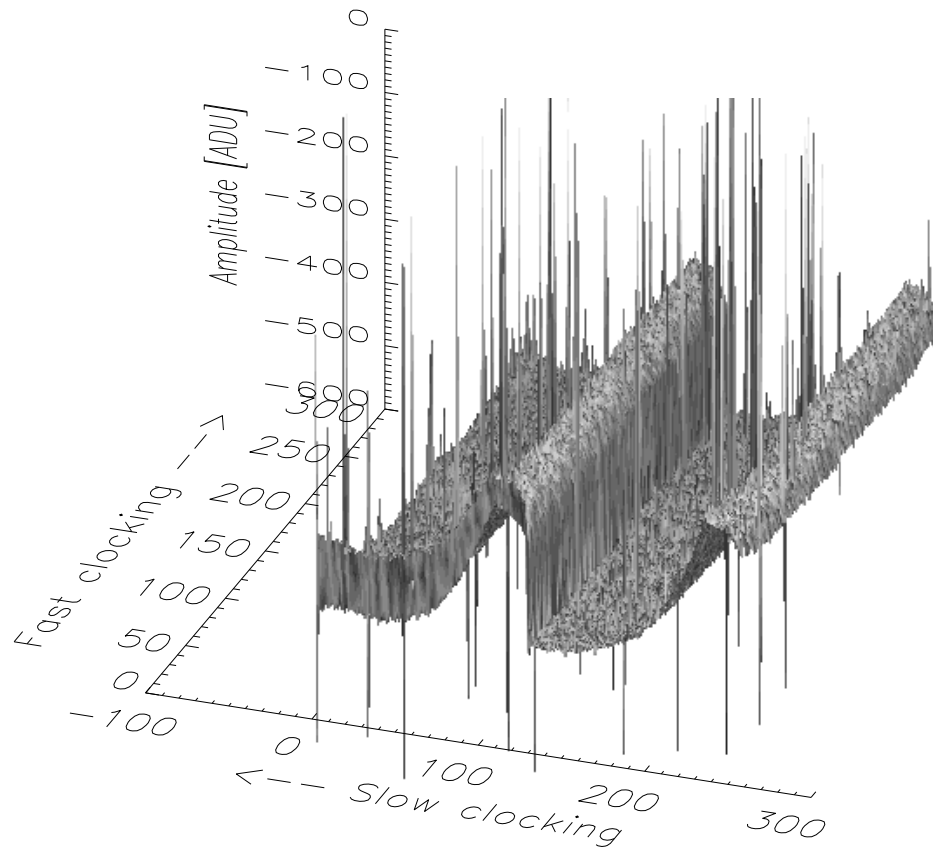


**Figure 1:** amplitude of the shading function for the Camera 2 detector. The gradient of the signal in the slow clocking direction is dramatic, while the gradient in the fast clocking direction, smaller by a factor 128, is difficult to see. Many bad pixels are seen very clearly; row 1 of the bottom left quadrant is bad (pixels 1 to 128 of row 1 in the fast clocking direction).

The shading signal is not the same for each readout. Its amplitude and to some extent its shape are a function of the time since a pixel was last read out (**not** reset). So readouts with the same DELTATIM (this is the keyword used in NICMOS data to denote the time since the previous readout) will have the same bias signal, for a given pixel. The dependence of this bias on DELTATIM is nearly logarithmic and quite repeatable, although there are some circumstances when this is not the case (namely in the MIF sequences it has been seen in on-orbit data that when changing from a very long DELTATIM to a very short one, the shading is not quite what is expected).

It is possible to find a numerical fit to the shading function in DELTATIM for each pixel of each detector. Thus it is (in principle) possible to predict what the bias signal is in any given pixel for **any** possible readout sequence. Another way to attack the problem is to make an average image of the bias for each of the DELTATIMs in the predefined MULTI-

ACCUM sequences. Then to build a synthetic dark, the bias component can be had by using the bias image for each appropriate DELTATIM in the sequence:

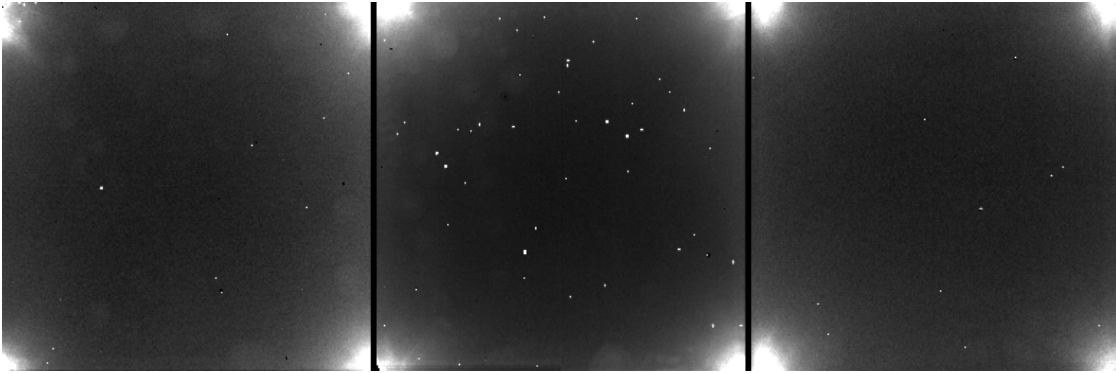


**Figure 2:** Amplifier glow images generated from on-orbit darks for all three NICMOS cameras. Camera 1 is on the left, and Camera 3 on the right. The bright spots in the central regions of the detectors are bad (hot) pixels.

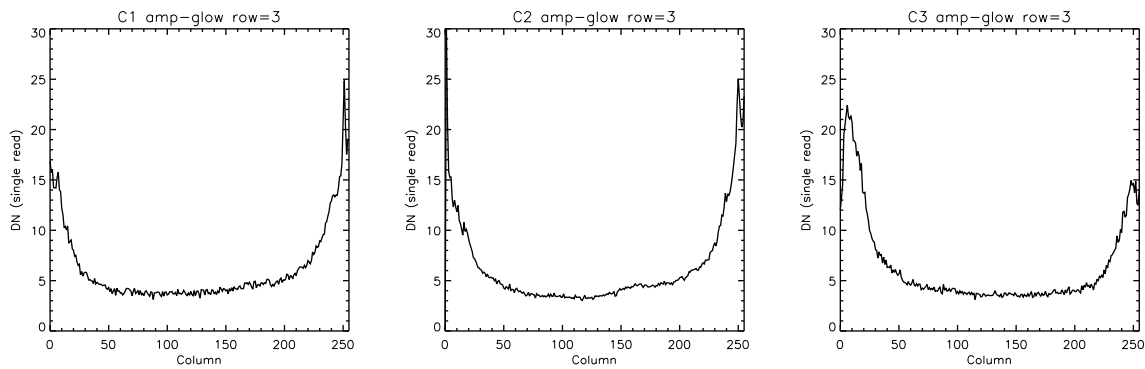


**Figure 3:** Slices along row 3 of the amp-glow images, close to the bottom where the amp-glow reaches its maximum, for Camera 1 (left) to Camera 3 (right) as above.

$$B(i,j) = S(i,j,DELATIM)$$

where  $S$  is the bias signal in a given pixel as a function of DELTATIM. It is the latter operation which is currently used in generating our synthetic darks.

### ***Linear Dark Current***

The linear dark current component is the traditional observed detector dark current when no outside signal is present. This component scales with exposure time only:

$$D(i,j) = T * d(i,j)$$

Where  $D(i,j)$  is the observed dark current signal in pixel  $i,j$  for a given readout,  $T$  is the

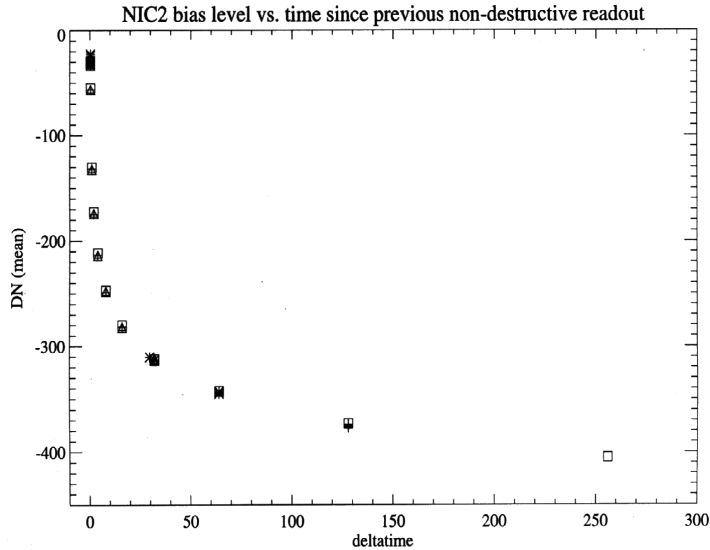


**Figure 4:** Shading amplitude (in ADUs) plotted against DELTATIM for a single pixel in Camera 2. The different symbols refer to different MULTIACCUM sequences. It is clear that for all the different sequences, the shading is a function of the DELTATIM, and so is unrelated to the time since last reset of the pixel.

time since the last detector *reset*, and  $d$  is the dark current (in  $e^-/\text{sec}$ ). The NICMOS dark current is extremely small and is very difficult to measure. It is approximately  $0.05 e^-/\text{s}$  over most of the area of each detector, rising to about twice this value close to the corners.

### 3. On-orbit Measurements of the Dark Characteristics

The challenge in calibrating these dark components for NICMOS detectors is disentangling the three components so that each can be measured independently of the other. Fortunately each component has entirely different sets of dependencies, and this can be used, along with the flexible way the NICMOS detectors can be operated, to achieve our goal.

First we note that the amp-glow is dependent only on number of readouts since the last detector reset. This means that to calibrate the amplifier glow, we need to find images with identical shading components but different number of readouts. Because of the dependence of shading, this turns out to be easy: if we look at any of the STEPxxx MULTIACCUM readout sequences, we find that after a set of logarithmically increasing DELTATIMs, they settle to a constant DELTATIM. For example, in the case of the STEP256 sequence, after an exposure time of 256 sec, readouts occur every 256 sec, and thus the shading is identical for each of these linearly spaced readouts. In this linear regime, the difference between the  $n$ th and the  $n+1$ th readouts is simply the signal added by 1 readout's worth of amp-glow (ignoring the dark current). Taking a full set of  $m$  linearly spaced readouts yields  $m$  lots of amp-glow, and thus obtains the highest S/N for the

resulting amp-glow image. Finally, to correct the amp-glow images for the small effects of the linear dark current, we can compare the amp-glow images generated as above using many different STEPxxx readout sequences, and use the difference in

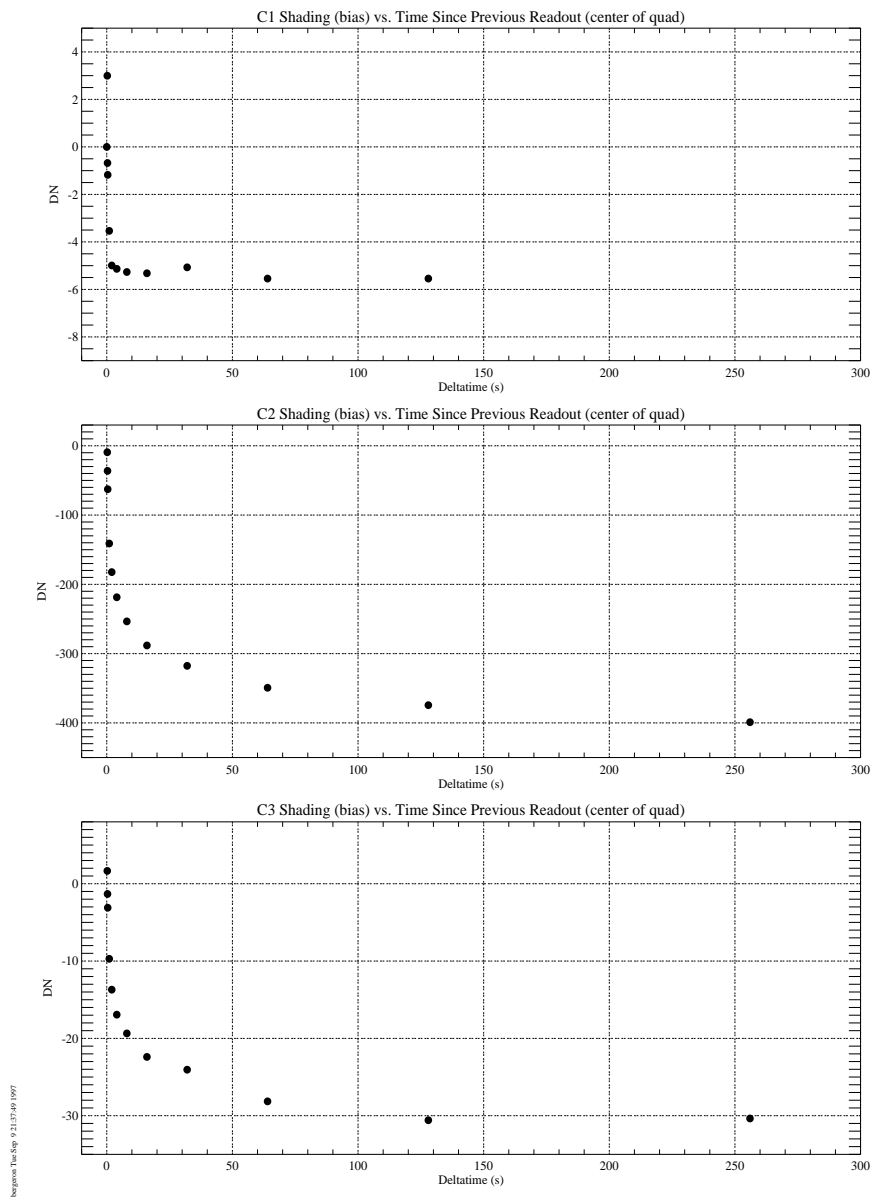


**Figure 5:** Amplitude of the shading signal vs. DELTATIM for a single representative pixel at the center of a quadrant for each of the three detectors.

DELTATIMs to measure the linear dark current. The resulting amp-glow images for all three cameras are shown in Figure 2, and cross sections through them along row 3, near the bottom of the image, are shown in Figure 3.

In order to measure the shading, first we correct each read of a MULTIACCUM exposure for amp-glow, using the amp-glow calibration images obtained above. Having removed

this component, shading is now the dominant remaining component. If we plot the amplitude of the shading signal against DELTATIM, we find the two are very strongly correlated (see Figure 4). In fact, the shading amplitude is dependent only on DELTATIM, and has **no** dependence on time since last reset whatsoever. This is illustrated by the fact that if we find any read in the STEP16 pattern whose DELTATIM is 16 seconds, for example, the shading amplitude for the same pixel of the same detector will be identical for a read from the STEP256 pattern for which DELTATIM is 16 seconds - regardless of how many reads have occurred previously in either observation.

In Figure 5 we plot the shading amplitude against DELTATIM for a pixel near the center of a quadrant, using observations made using many different MULTIACCUM sequences.

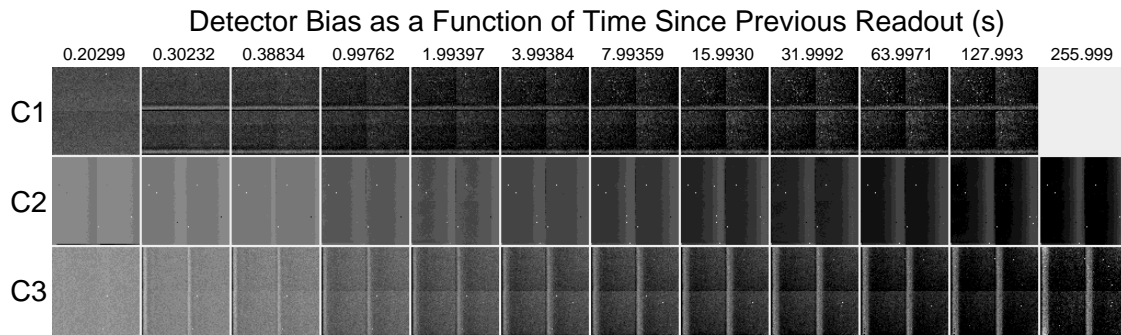


**Figure 6:** Images of the shading for each of the three cameras as a function of DELTATIM (indicated at the top in seconds).

Figure 6 shows the shading image as a function of DELTATIM for all three cameras. The detectors are mounted in the cameras such that the readout directions are rotated by multiples of 90 degrees with respect to one another, and so the shading patterns in Cameras 2 and 3 run parallel to one another, while that for Camera 1 is in the orthogonal direction. In Camera 1 the shading generates a bright band along the first row to be read out of each quadrant, parallel to the time axis in Figure 6. In Camera 3 a similar bright band is generated, but now the band runs orthogonal to the time axis of Figure 5. Note that the shading generates a large **negative** signal. The gradient of the shading function is seen to be quite steep in the direction orthogonal to the bright bands seen in Cameras 1 and 3: this direction is the ‘slow clocking direction’, as the time between pixel readouts in this direction is 128 times a single pixel readout time. In the orthogonal direction, the ‘fast clocking direction’, it is more difficult to see the gradient in the shading - but it can be seen in Camera 3 by virtue of the quadrant boundaries.

In order to give an impression of the amplitude of the shading function, we have generated an average shading function (for display purposes only) by taking, for each Camera, a median of the pixel values along a row parallel to the fast clocking direction. Taking a median rather than a mean effectively filters out bad pixels. The resulting shading functions are plotted in Figure 5 for each of the DELTATIMs for which images are plotted in

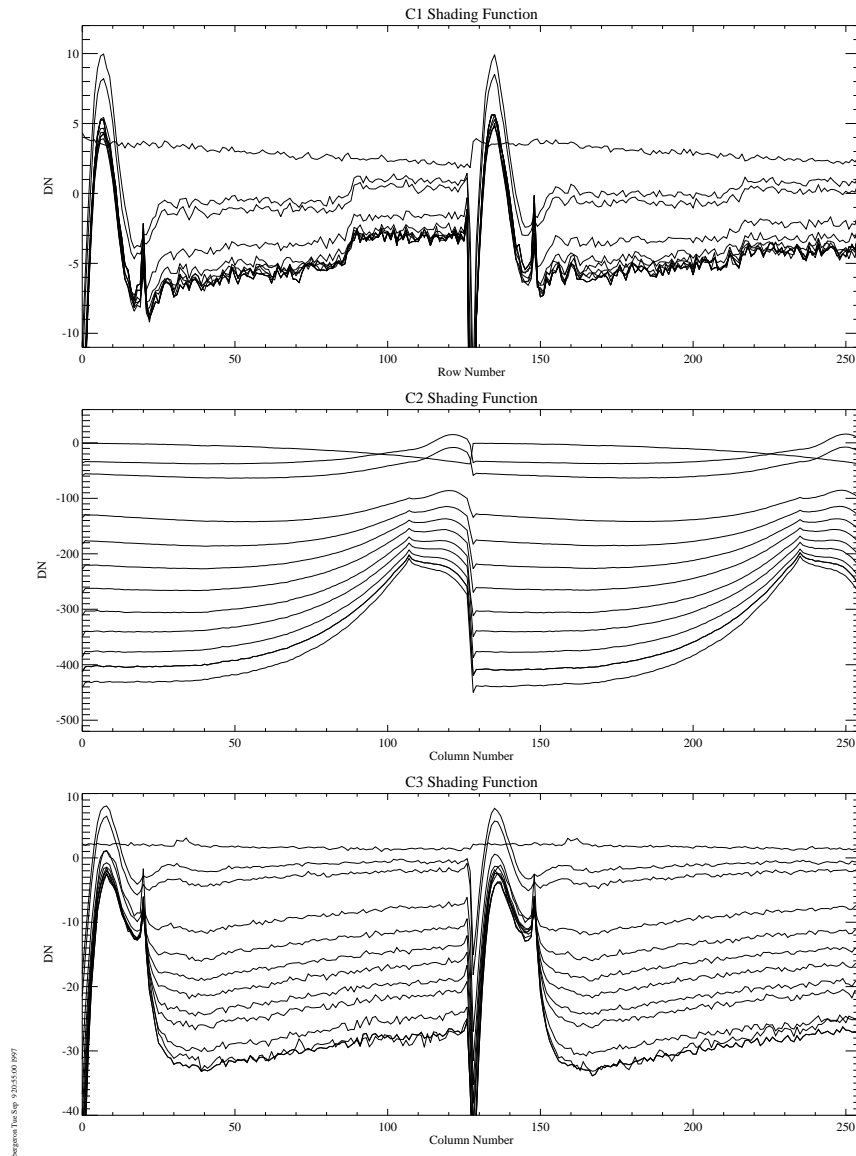


**Figure 7:** Representative shading functions for the slow clocking direction for each of the three detectors. These have been generated by taking medians along the fast clocking direction in order to improve S/N while filtering out bad pixels.

Figure 6. A number of effects are seen readily in this figure. First, the progression of curves heading towards increasingly more negative values shows how the shading amplitude changes with increasing DELTATIM. Second, the strong gradient in shading amplitude in the slow clocking direction is seen very clearly. Third, the fact that Cameras 2 and 3 are rotated 180 degrees with respect to one another shows up because the time axis along the slow clocking direction is reversed - and thus the shading function is exactly reversed in Camera 2 compared with Camera 3. Fourth, the spike seen in the 20th row for each quadrant of each Camera (because Camera 2 is reversed, it is the 108th row for this

Camera) is a result of the way the readouts are carried out: for a variety of reasons, the first 20 rows are read out a first time but the results discarded, and then the whole 128 rows are read out and the results recorded. This means that at the 20th row there is a large discontinuity in the time since last read, and thus the shading pattern exhibits rather extreme behavior at this location. Fifth, in each Camera the top curve is seen to be rather anomalous, the gradient in many cases being reversed with respect to all the other curves: this curve is that for the SCAMRR sequence, which has reads separated by only 0.203 seconds (exactly the time taken to read the whole detector once), and which can only be used when only one camera is in use. The reason the shading is so different for this sequence is not known, but the observation is probably important. Sixth, for Camera 1 ‘jumps’ are present in the shading function near rows 85 for each quadrant: again, the reason for this is currently unknown, but the effects are very clear in observations.

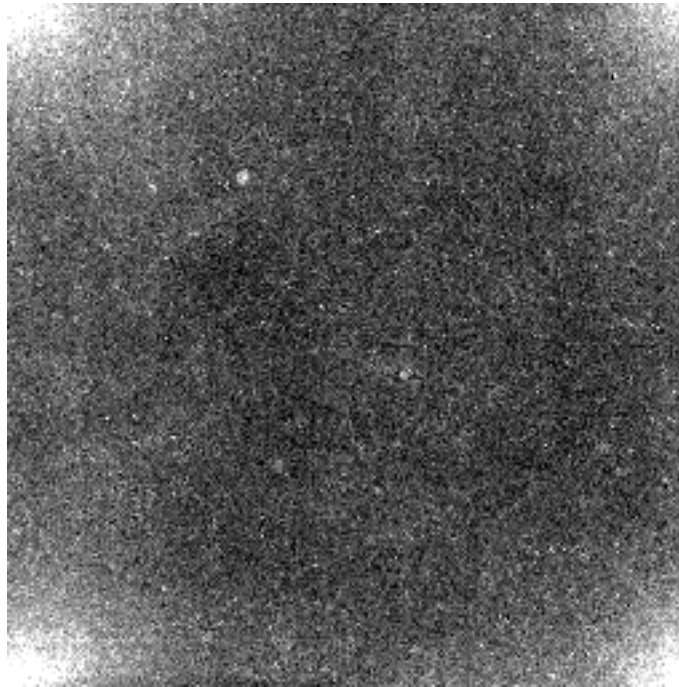


**Figure 8:** image of the true, ‘linear dark current’, for Camera 2. The amplitude is about  $0.05e^-/\text{sec}$  over most of the detector, rising sharply near the corners to roughly  $0.1e^-/\text{sec}$ .

The linear dark current can be measured in a number of ways. The technique which was used initially was to derive, for a number of MULTIACCUM sequences for which high quality on-orbit darks were obtained, synthetic dark current images using the amplifier glow and shading contributions as determined above. These were then subtracted from the

observations. The residual was seen for Camera 2 to be a very low amplitude signal increasing roughly linearly with time. This was the linear dark current. The mean across

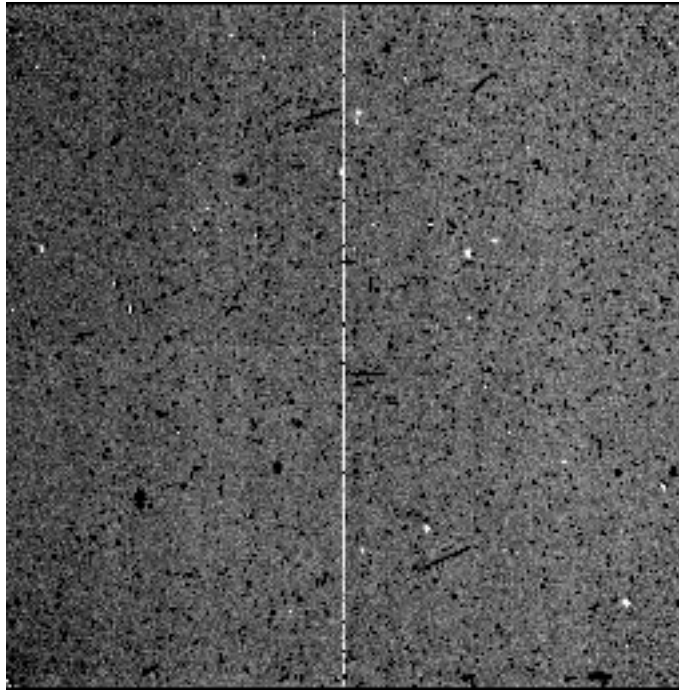


**Figure 9:** Image of the difference between an averaged set of on-orbit darks for the STEP8 MULTI-ACCUM sequence and the corresponding synthetic dark, for the 22nd readout. Note the ‘photometrically challenged’ column 128.

the whole detector was determined in order to get moderate S/N. For Cameras 1 and 3 no residual could be seen above the uncertainties, indicating that the dark current is very small for these two cameras.

A better technique which has recently been put into practise is to measure the amplifier glow signal, as described in section 3, for a section of a STEPxxx MULTIACCUM observation involving linearly spaced darks. This is done for a number of different MULTIACCUM patterns. The different patterns, because they involve different total integration times, contain different linear dark current contributions, and thus the ‘amplifier glow’ measurements will differ. By comparing the results from the various different sequences, the linear dark current can be estimated. It is found that the linear dark current is not uniform across the detector, but is much larger in the corners, in a manner qualitatively similar to the amplifier glow images. However, in the case of the dark current, the image is in fact fairly flat across much of the detector, with the increased dark current being seen only in regions within roughly 30 pixels or so of the corners. For Camera 2, we find by this technique that the dark current is roughly  $0.05e^-/\text{sec}$  across most of the array, rising to about  $1.0e^-/\text{sec}$  in the corners (the Camera 2 dark image is shown as Figure 8). This result is nicely consistent with the value obtained from the previous technique. Simi-

lar results are obtained for the other two cameras. The synthetic darks delivered to CDBS up to October 1997 assumed a uniform linear dark current. As a result, in longer exposures the dark signal in the corners of the detectors was often underestimated, giving rise to what looked like residual amplifier glow in the calibrated data. We now know thta this was

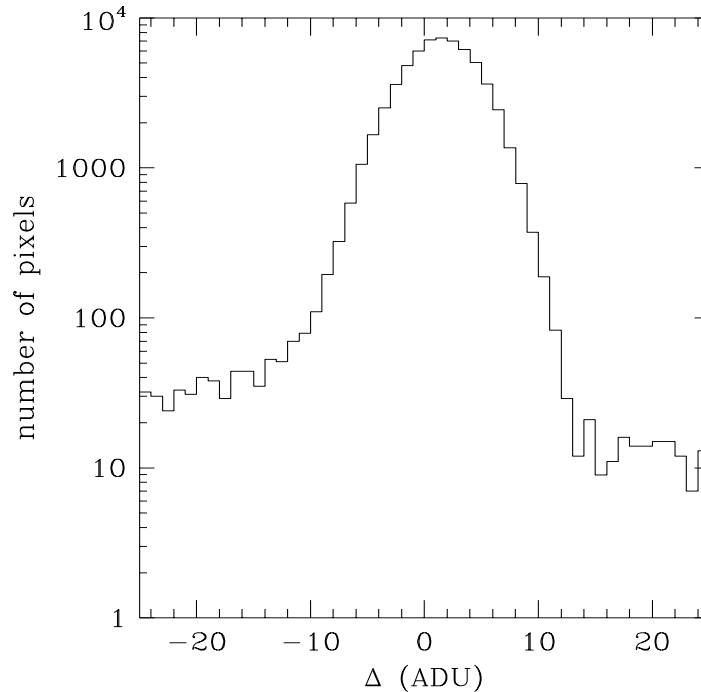


**Figure 10:** Histogram of the pixel values in the difference image displayed in Figure 9.

in fact real dark current structure, not amplifier glow, and the most recent synthetic darks no longer suffer this effect.

#### 4. Making a Synthetic Dark

The total “dark” signal in any given pixel of any given NICMOS MULTIACCUM readout is just the sum of the 3 components described above:

$$DARK(i,j) = D(i,j) + A(i,j) + B(i,j)$$

An IDL routine has been developed to make synthetic darks. This routine uses the amplifier glow image displayed in Figure 2 and 3, and simply multiplies it by the accumulated number of reads in order to generate  $A(i,j)$  for each readout. The shading as a function of DELTATIM has been populated by the technique described above, yielding an array of shading images some of which are displayed in Figure 6. An appropriate image is picked out of this array in order to generate  $B(i,j)$  for each readout. Finally, the linear dark current is determined using the dark images measured as described above (and plotted in Figure 8 for Camera 2) multiplied by the exposure time at each readout. Finally, the routine now

sums the three contributions for each readout.

The calibration database has been populated with MULTIACCUM darks for all sequences which have not yet been observed on-orbit, or for which other effects, such as the pedestal, have contaminated the early on-orbit dark observations. There are plans to tune up the synthetic dark algorithm somewhat (see next section) and eventually release it as an STSDAS tool in the NICMOS package.

## 5. How Good Are The Synthetic Darks?

Comparisons of on-orbit to synthetic darks show that the differences are relatively small - usually of the order of a few ADUs, with the largest differences in the corners of the detectors. We believe that most of the differences we now observe between on-orbit darks and our synthetic darks are a result of temperature fluctuations of the detectors. These will be described in more detail in a future ISR, but we note here that the shading function for each pixel is seen to be quite sensitive to detector temperature, that the linear dark current is very sensitive to detector temperature, and that the temperature appears to vary during the course of typical exposures, as well as varying significantly with spacecraft attitude and other environmental factors. As an example, we show here the difference between a synthetic STEP8 dark calibration reference file, and a STEP8 reference file generated as the mean of a set of 8 22 readout STEP8 dark observations obtained as part of the 7116 ERO observation. The observed dark contains a few hundred Cosmic Rays which were not successfully median filtered out when the individual exposures were combined. (Overall we would expect to have received about 2000 Cosmic Ray hits in the set of darks; most of these have been successfully removed by the combination algorithm, with about 10-20% of them remaining, mostly because their amplitude was too low to be detected.) These can be seen in the difference image of the 22nd readouts (Figure 9) as dark blobs or streaks. Overall we can see that there is no residual shading pattern in the difference image, and no residual amp-glow. There is about a couple of ADUs worth of residual linear dark current in the corners. There is a small gradient across the image from right to left, with an amplitude of about 1ADU. However, the residual signal is very small. The histogram of pixel values in the difference image, which is shown as Figure 10, shows that the modal difference is about 1ADU between the observed and synthetic dark. The difference images for the intermediate readouts look similar, with very little structure visible in them apart from a small amount of residual linear dark current in the corners in some. This is fairly typical of most of the MULTIACCUM sequences, the synthetic darks in general reproducing quite faithfully the observed behavior. The bright column seen in Figure 7 is column 128. This has been dubbed the 'photometrically challenged' column: it frequently displays a level that is offset from the rest of the image, and the offset has been suggested anecdotally to have an amplitude that is greater in pedestal impacted data. The reason for the offset in column 128 is not known.

The ‘pedestal’ effect also adds some uncertainty to the on-orbit data used in these comparisons. This effect was first seen during SLTV, but not understood, and has been seen frequently in on-orbit data. It is typically seen after a detector has spent some time in autoflush mode, and manifests itself as a bias offset which decays pseudo-exponentially with time. The pedestal will be described in a forthcoming ISR (Bergeron & Skinner, in preparation). Although every effort was made to throw out pedestal-affected data when making the reference files currently in the database, some pedestal may nonetheless be present in either the synthetic darks generated as described here or in the on-orbit darks with which we are comparing them, so very accurate comparisons will be difficult until such time as the pedestal is either eliminated from the instrument or can be accurately calibrated by other means. It may be possible eventually to generate code which can automatically detect and remove the pedestal effect from data. Since we are currently at an early stage in our understanding of the pedestal, such code does not yet exist. A routine which appears to be able to remove the pedestal fairly successfully from some types of data has been developed, and is currently being tested, but its effectiveness is not yet sufficiently well understood to use it in this analysis.

There is also a problem with proper shading correction in the first of the multiple readouts at the end of the MIFxxx sequences. This single readout is the only time a shorter DELTA-TIM occurs after a longer one in the defined sequences, and is somehow affected by this. The result is a lower amplitude shading function than expected for this readout. The difference amounts to 50-100 ADUs in a smooth gradient across a given quadrant in the readout direction, indicating a change in function shape for that readout. All previous and subsequent readouts appear unaffected. After CALNICA combines all the readouts to make the final calibrated image, the effect of this one imperfect dark frame will be rather small - in fact, it is likely to fool CALNICA into registering Cosmic Ray hits for most of the pixels in this one readout, and therefore ignoring that read for those pixels when assembling the final calibrated image. The most recent version of the synthetic dark code now models this effect, and at the time of writing the first synthetic darks from this improved code have just been delivered to CDBS for use by the calibration pipeline.

Provided the above issues can be resolved, the synthetic darks offer large advantages compared to dark calibration reference files generated by more traditional reduction of on-orbit darks of the same MULTIACCUM sequence. The biggest advantage is S/N. As can be seen from Figure 5, the amplitude of the combined dark signal is rather low. The read noise for the flight detectors is approximately 6ADUs, and so obtaining good S/N on the darks requires many observations, each of which may be quite time consuming. Because the synthetic dark approach applies observations made in many different MULTIACCUM sequences to each component of the dark, S/N comparable with that which can be obtained in a complete on-orbit calibration of all MULTIACCUM sequences can be obtained in far fewer orbits. Alternatively, one can make a complete set of observations, but by combining them in this way one can obtain much higher S/N reference files, and

thus better calibrated data. Intermediate approaches are also of course possible.

The presence of the 'pedestal' effect has greatly impacted the Cycle 7 dark current calibration program, by seriously altering the behavior of the detectors during some of the observations in the program. These observations are then not used in the subsequent reference file generation, thus degrading the S/N. Using synthetic darks either instead or in concert with the calibration program observations, has greatly alleviated this problem. In general the greatest problem faced in the dark calibration at present is the pedestal effect, and we will address this effect in a subsequent ISR.